Local Density Discrete Variational Xα Calculations on Transition-metal Oxycation Complexes: d–d and Charge-transfer Spectra of Molybdenyl Species *

Robert J. Deeth
School of Chemistry, University of Bath, Claverton Down, Bath BA2 7AY, UK

Theoretical d–d and charge-transfer electronic transition energies for the structurally characterised d^1 MoO^{3+} complexes $[MoOCl_4]^-$, $[MoOCl_4(OH_2)]^-$, $[MoOBr_4(OH_2)]^-$, $[MoOF_5]^{2-}$ and $[MoO(NCS)_5]^{2-}$ are reported and compared with the most recent experimental data. The discrete variational Xα model gives excellent reproduction of band energies and assignments for each individual complex and for the whole series. With two minor exceptions, the experimental and theoretical results are in agreement and support the general validity of the Ballhausen–Gray picture of the electronic structure of d^1 oxycation species.

Metal oxycations, MO_m^{n+}, dominate the chemistry of the early members of all three transition-metal series.[1] In particular, oxycations are crucial for a variety of important oxygen-transfer reactions[2] and are implicated in the biochemistry of vanadium and molybdenum.[3] The electronic structures of d^1 oxometal species MO^{n+} have been actively studied since the pioneering molecular orbital (MO) treatment of the VO^{2+} ion in $[VO(OH_2)_5]^{2+}$ by Ballhausen and Gray.[4] Soon after, Gray and Hare[5] extended the treatment to CrO^{3+} and MoO^{3+} complexes, concluding that the electronic structures of all three oxycation systems were broadly the same. This view was later challenged on experimental grounds by Garner *et al.*[6] More recently, however, the exacting and comprehensive spectroscopic measurements by Collison and co-workers on VO^{2+},[7] CrO^{3+} (ref. 8) and MoO^{3+} (ref. 9) species have apparently established the essential validity of the Ballhausen–Gray (BG) scheme.

Spectra for these d^1 MO^{n+} species have, in many cases, been measured at low temperatures using single crystals and polarised light. The observation of vibrational fine structure often leads to an unambiguous assignment of the transition and a uniform description of the electronic structures of d^1 MO^{n+}systems has emerged.[7–9] Hence, the first two bands in the absorption spectrum are usually d–d in origin, except for some MoO^{3+} species with very soft ligands like Br where the second of these bands is a low-energy charge transfer (c.t.) transition.[9] The third band may be d–d or c.t. in nature. For example, it is a d–d feature for $[CrOCl_4]^-$ (ref. 8) and five-co-ordinate VO^{2+} complexes[7] while for six-co-ordinate VO^{2+} species the third band is a c.t. absorption.[7]

Theoretical analyses are not yet in such general accord. The original study of VO^{2+} was only based on a relatively crude semiempirical MO method.[4] A later, improved treatment,[10] while predicting rather different transition energies, did still largely support the earlier work. In contrast, more sophisticated all-electron multiple scattering Xα (MSXα) calculations on $[CrOCl_4]^-$ and $[MoOX_4]^-$ (X = Cl or Br),[11] and *ab initio* configuration interaction (c.i.) results for $[CrOCl_4]^-$,[12] predict the second band of the chromium molecule to be a c.t. process. However, these two studies suggest different assignments for this absorption. A second MSXα treatment[13] apparently supports the BG scheme although only the d–d transition energies were computed. None of the above approaches agrees satisfactorily with the very latest spectroscopic data on MO^{n+} species. On the other hand, the discrete variational Xα (DVXα) model gives near-quantitative reproduction of the d–d and c.t. spectra of $[CrOCl_4]^-$ (ref. 14) and the d–d spectra of six diverse VO^{2+} molecules.[15] Importantly, it predicts the correct assignments as well as accurate transition energies.

The present work completes the picture by examining the electronic structures of MoO^{3+} species. Once again, Collison[9] provides an excellent source of detailed experimental data. The d–d and c.t. transition energies are computed for $[MoOCl_4]^-$, $[MoOCl_4(OH_2)]^-$, $[MoOBr_4(OH_2)]^-$, $[MoOF_5]^{2-}$ and $[MoO(NCS)_5]^{2-}$. In common with the previous DVXα studies, excellent agreement with the experimental data is obtained. With one or two minor modifications, the DVXα results confirm the conclusions drawn from spectroscopic measurements and the essential validity of the Ballhausen–Gray model. The successful treatment of MoO^{3+} complexes paves the way for future studies of other molybdenum oxycation species especially d^2 MoO^{2+} and d^0 MoO_2^{2+} systems implicated in oxygen-transfer reactions relevant to molybdenum biochemistry.

Computational Details

The density functional formalism[16] provides, in principle, a method for calculating the ground-state electron density *exactly*, *i.e.* including all possible electron-correlation effects. Unfortunately, it does not indicate the exact form of the appropriate functional, merely that one exists. In practice, therefore, various approximate approaches have been developed. In chemistry, the so-called local-density Xα methods are probably the best known. The DVXα model is a numerical, local-density scheme with which considerable success has been achieved for transition-metal systems. The method has been described elsewhere[16] and only those details relevant to the present study are included here.

Spin-restricted DVXα self-consistent charge (SCC)[17] calculations have been carried out using near-minimal single-site-orbital (SSO) basis sets[18] (up to 5p on Mo, up to 2p on F, O, N and C, up to 3p on S and Cl, up to 4p on Br and 1s on H). The core functions (up to 4p Mo, 1s on F, O, N and C, up to 2p on S and Cl and up to 3p on Br) were frozen and orthogonalised against the valence orbitals.[19] The SSO basis sets were further constrained by applying an external potential

* *Supplementary data available* (No. SUP 56831, 5 pp.): molecular orbital energies and atomic orbital compositions. See Instructions for Authors, *J. Chem. Soc., Dalton Trans.*, 1991, Issue 1, pp. xviii–xxii.
Non-SI units employed: au $\approx 5.29 \times 10^{-11}$ m, eV $\approx 1.60 \times 10^{-19}$ J.

Table 1 Structural parameters for molybdenyl complexes

Complex	Distances (Å)			Angle (°)	
	Mo–O	Mo–L_{eq}	Mo–L_{ax}	O–Mo–L	Ref.
$[MoOCl_4]^-$	1.610	2.333	—	105.25	23
$[MoOCl_4(OH_2)]^-$ [a]	1.672	2.359	2.393	99.0	24
$[MoOBr_4(OH_2)]^-$ [a]	1.656	2.529	2.337	97.69	25
$[MoOF_5]^{2-}$	1.71	1.945	1.99	95.6	26
$[MoO(NCS)_5]^{2-}$ [b]	1.646	2.055	2.228	97.27	27

[a] O–H 0.98 Å, H–O–H 107°. [b] N–C_{eq} 1.157, C–S_{eq} 1.601, N–C_{ax} 1.127 and C–S_{ax} 1.636 Å.

well of depth −2au, with inner and outer radii of 4 and 6 au respectively for Mo, S, Cl and Br and 2 and 4 au respectively for the other atoms. The bases were optimised for each molecule as previously described.[20]

The three-dimensional grid of sampling points used in the numerical integrations was arranged such that *ca.* 1500 points were associated with Mo and between 600 and 800 points each for the remaining atoms. This distribution scheme ensures a numerical error of approximately ±0.02 eV in molecular orbital (MO) energies and ±0.005 in atomic orbital populations, relative to the limit of a very large number of sampling points. All charge densities and orbital populations were based on Mulliken analyses.[21] Estimates of the transition energies were computed using Slater's transition-state formalism.[22]

The structural parameters used in the DVXα calculations are presented in Table 1. They were derived from X-ray structural studies on $[AsPh_4][MoOCl_4]$,[23] $[AsPh_4][MoOCl_4(OH_2)]$,[24] $[NEt_4][MoOBr_4(OH_2)]$,[25] $[NH_4]_2[MoOF_5]$[26] and $[NMe_4]_2[MoO(NCS)_5]$.[27] Symmetries have been slightly idealised to C_{4v} or C_{2v} as appropriate. For the C_{4v} molecules the *xz* and *yz* planes contain the Mo–L_{eq} vectors, where L_{eq} refers to an equatorial ligand, while for the C_{2v} molecules these planes bisect the Mo–L_{eq} vectors. The water molecules lie in the *xz* plane. The NCS ligands in $[MoO(NCS)_5]^{2-}$ are assumed to be linear with linear Mo–NCS bonds.

Results and Discussion

Theoretical treatments of MoO^{3+} species are relatively rare. Gray and Hare[5] have performed for $[MoOCl_5]^{2-}$ a semi-empirical MO analysis similar to the Ballhausen–Gray treatment of $[VO(OH_2)_5]^{2+}$. In addition, there are two MSXα studies[11,13] which deal with $[MoOCl_4]^-$. Sunil *et al.*[13] also include MSXα calculations on a variety of other d^1 oxometal complexes and their results on $[MoOF_5]^{2-}$ are of relevance here. The overlapping-spheres MSXα and DVXα SCC methods give comparable results.[20] However, the choice of the extent of overlap in the MSXα approach is subjective[28] while in the DVXα SCC scheme it is determined self-consistently. Although the overall electronic structures are therefore broadly similar, the DVXα SCC method generally gives a superior description of the spectroscopic transition energies than does the MSXα approach. Moreover, in those cases where the SCC procedure is inadequate, there is a well defined path for progressively improving the accuracy of a DVXα calculation.[29] Such a path is not available within the MSXα scheme.

Ground-state Electronic Structures.—All calculations on MoO^{3+} species, including the present DVXα results, predict that the unpaired electron is housed in the essentially d_{xy} orbital for the C_{4v} molecules or in $d_{x^2-y^2}$ for the C_{2v} molecules. The predicted d-orbital sequence is always $d_{xy} < d_{xz},d_{yz} < d_{x^2-y^2} < d_{z^2}$ for C_{4v} species or $d_{x^2-y^2} < d_{xz},d_{yz} < d_{xy} < d_{z^2}$ for the C_{2v} aqua complexes. The nature of the MOs for all the molecules studied here is fairly similar and comparable to those already reported[14] for $[CrOCl_4]^{2-}$ in terms of the compositions and relative energies of the halide functions, metal–oxo bonding levels and the metal d orbitals. Table 2 illustrates the case for $[MoOCl_4]^-$ while the data for the other complexes have been deposited as SUP 56831. The highest-occupied molecular orbital (HOMO) ($2b_2$) contains the unpaired electron leading to the correct $^2B_2$ ground state. The levels immediately above (6e to $6a_1$) are of mainly d-orbital character. Just below the HOMO comes a set of ligand-based levels, $1a_2$ to $4a_1$, derived largely from the equatorial donors. Below the equatorial ligand MOs come the main Mo–Cl ($1b_2$ to $2b_1$) and Mo–O ($3a_1$ and 2e) bonding levels with the remaining lower-energy functions ($1b_1$ to $1a_1$) being mainly ligand-based s orbitals. The latter do not participate appreciably in the bonding.

The main difference between the electronic structure of $[MoOCl_4]^-$ and those of the other molecules relates to the MOs for the axial ligand *trans* to the molybdenyl oxygen. For $[MoOF_5]^{2-}$ and $[MoO(NCS)_5]^{2-}$ the MOs are just below the HOMO but *above* those from the equatorial donors, while for the aqua complexes the axial ligand MOs appear *below* the equatorial ligand levels.

With the exception of the NCS complex, the main Mo–O σ- and π-bonding interactions are concentrated in individual functions. Plots of the relevant σ-bonding MOs for each halide complex are depicted in Fig. 1 with the π functions shown in Fig. 2. There are large σ and π interactions between the Mo atom and the oxygen consistent with multiple Mo–O bonding. The nodal behaviour of the combining atomic orbitals is also apparent. One interesting feature of Figs. 1 and 2 is the tendency of the Mo–L_{eq} interaction to be directed towards the centroid of the MoO electron density rather than directly at the Mo atom. This effect is most pronounced for $[MoOCl_4]^-$ and $[MoOF_5]^{2-}$. The oxometal species appears to behave more as an integrated unit rather than as separate atoms which squares well with the stability of the molybdenyl unit.

For the six-co-ordinate species there is another important facet displayed in the figures. One notes that for the aqua complexes the $H_2O \rightarrow MoO$ interaction is antibonding while for $[MoOF_5]^{2-}$ the $F \rightarrow MoO$ interaction is bonding. [An examination of the wavefunction for $[MoO(NCS)_5]^{2-}$ shows the same feature as for the fluoride complex but spread over several MOs.] This correlates with the location of the MOs of the sixth ligand relative to the HOMO as described above and has important consequences for the interpretation of the electronic spectrum (see below).

Metal–Ligand Bonding.—A detailed picture of the metal–ligand bonding can be obtained from a Mulliken analysis of the DVXα ground-state charge densities. Computed gross charges and overlap populations are collected in Table 3. Both the Mo–O charges and the Mo–O overlap populations for the six-co-ordinate species correlate directly with the Mo–O bond lengths. Hence, as the Mo–O distance increases in the sequence $[MoO(NCS)_5]^{2-} < [MoOBr_4(OH_2)]^- < [MoOCl_4(OH_2)]^- < [MoOF_5]^{2-}$, so too does the total MoO charge while the overlap decreases in the same sequence. The latter correlation also extends to $[MoOCl_4]^-$ which has the shortest Mo–O bond and the largest overlap of all the complexes studied here. Such correlations were not evident from the DVXα calculations on VO^{2+} complexes.[16] However, the latter considered a more complicated series of molecules than those treated here and it may well be that the smooth relationship found for the MoO^{3+} species results from analysing only simple halide and pseudohalide complexes.

The equatorial ligand charges do not appear to correlate with their expected donor properties. The charges vary as F < NCS ≤ Cl ≤ Br suggesting a stronger donor role for Cl and Br than for NCS. In contrast, the Mo–L_{eq} overlap

Table 2 Molecular orbital energies and their atomic orbital compositions for $[MoOCl_4]^-$

		Mo			O		Cl	
MO	*E*/eV	4d	5s	5p	2s	2p	3s	3p
$8a_1$	14.6207	19.4	9.6	60.7	3.7	5.2	0.1	1.3
7e	13.4931	0.1	—	91.6	—	1.9	0.9	5.4
$7a_1$	9.6338	−0.1	75.2	10.7	0.2	0.5	1.5	12.1
$6a_1$	4.6374	45.3	1.7	22.2	0.1	20.7	0.2	9.9
$4b_1$	3.6625	64.8	—	—	—	—	1.3	33.9
6e	2.8044	66.9	—	−0.1	—	22.9	0.2	10.1
$2b_2$*	0.8676	78.6	—	—	—	—	—	21.4
$1a_2$	−1.4455	—	—	—	—	—	—	100.0
5e	−2.0470	0.4	—	0.0	—	2.8	−0.1	96.8
$3b_1$	−2.1363	0.1	—	—	—	—	0.0	99.9
4e	−2.4327	0.0	—	0.0	—	7.7	0.0	92.3
$5a_1$	−2.9073	−0.1	0.2	2.8	0.5	10.5	0.0	86.1
3e	−3.4359	0.7	—	6.2	—	8.3	1.4	83.5
$4a_1$	−4.1379	0.1	8.5	1.8	0.8	13.4	2.8	72.7
$1b_2$	−4.1415	21.4	—	—	—	—	—	78.6
$2b_1$	−4.3809	31.1	—	—	—	—	3.2	65.7
$3a_1$	−5.1903	27.4	1.3	1.7	3.8	48.2	1.3	16.3
2e	−5.2642	31.3	—	0.8	—	56.4	0.3	11.2
$1b_1$	−14.3138	4.1	—	—	—	—	95.5	0.5
1e	−14.3342	0.6	—	1.4	—	0.0	97.3	0.7
$2a_1$	−14.8303	1.1	2.8	0.3	0.0	0.0	94.2	1.6
$1a_1$	−18.2565	6.9	0.8	−0.1	90.9	1.4	0.1	0.0

* HOMO.

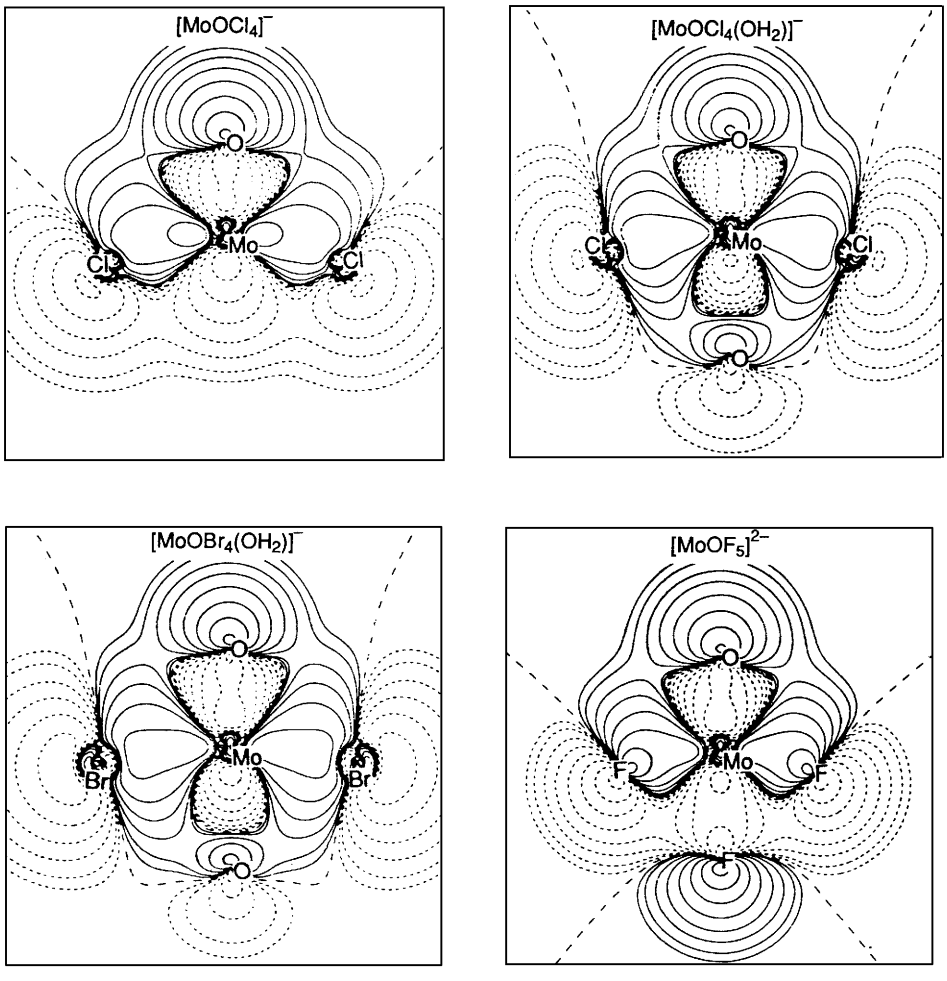

Fig. 1 Plots of main metal–oxygen σ-bonding MOs for molybdenyl halide complexes. Solid lines indicate positive contour values, short dashes negative and long dashes zero values. Successive contours differ by a factor of 2

populations vary as NCS > Br ≈ Cl > F, which squares much better with the expected chemistry of these ligands. Previous applications of the DVXα method[16,20,30] have also concluded that the overlap populations provide a more

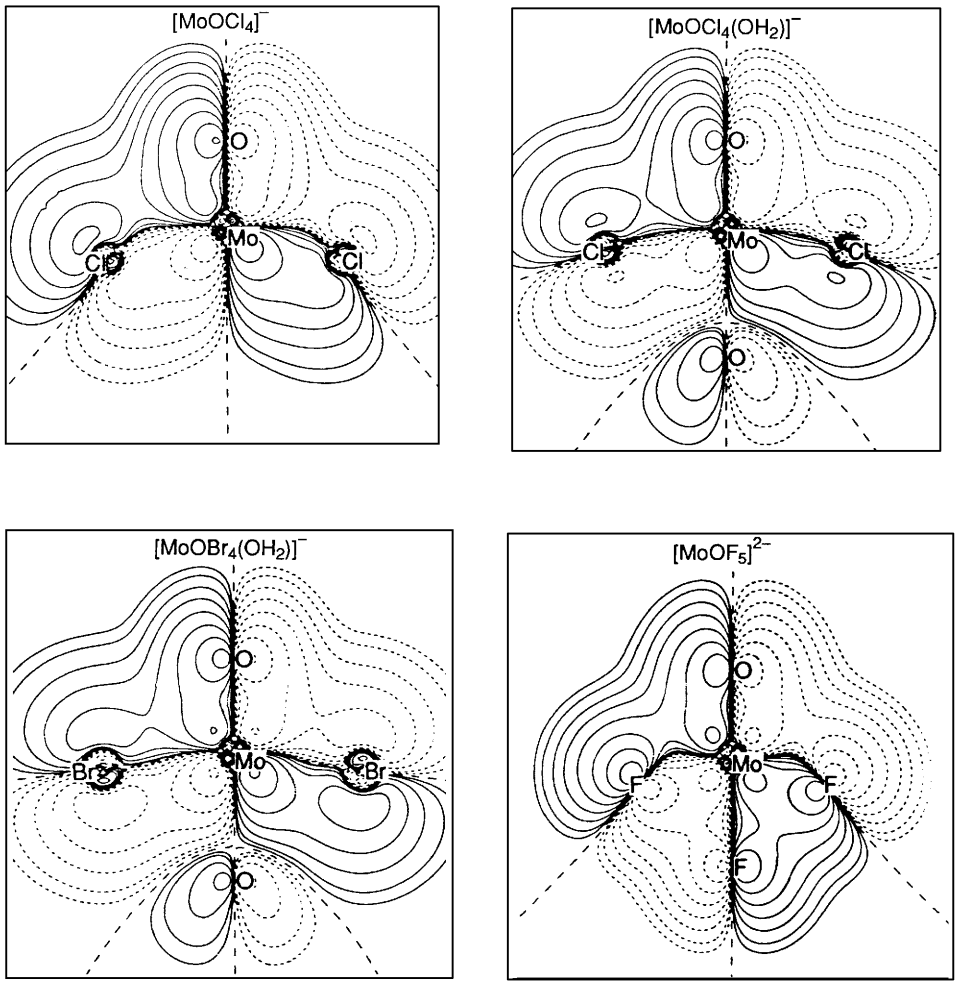

Fig. 2 Plots of main metal–oxygen π-bonding MOs for molybdenyl halide complexes. Contour line styles as in Fig. 1

Table 3 Gross charges and overlap populations

	Charge			Overlap			
Complex	MoO	L_{eq}	L_{ax}	MoO	Mo–L_{eq}	Mo–L_{ax}	Σ_{ov}
$[MoOCl_4]^-$	0.916	−0.479	—	1.025	0.442	—	2.794
$[MoOCl_4(OH_2)]^-$	1.000	−0.526	0.101	0.978	0.397	0.131	2.697
$[MoOBr_4(OH_2)]^-$	0.810	−0.476	0.134	0.995	0.437	0.113	2.856
$[MoOF_5]^{2-}$	1.276	−0.645	−0.696	0.877	0.274	0.238	2.209
$[MoO(NCS)_5]^{2-}$	0.790	−0.536	−0.645	0.998	0.526	0.360	3.471

consistent description of the M–L bonding than does gross atomic charge. The strength of the Mo–O π bond is shown by the π contribution to the Mo–O overlap being about twice as large as that of the σ component. A similar result obtains for $[CrOCl_4]^-$ (ref. 14) and vanadyl complexes.[15]

The metal–ligand overlaps for the donors *trans* to the molybdenyl oxygen are also collected in Table 3. For the aqua complexes the Mo–OH_2 overlaps of about 0.11–0.13 are around one quarter of the equatorial Mo–X (X = Cl or Br) values. This is consistent with the long Mo–OH_2 bond lengths of around 2.35 Å (see Table 1). On the other hand, the Mo–F_{ax} distance in $[MoOF_5]^{2-}$ is only about 0.05 Å longer than the Mo–F_{eq} contact and hence there is only a small drop (of about 0.04 or 13%) in the Mo–F_{ax} overlap. For $[MoO(NCS)_5]^{2-}$ the axial Mo–NCS distance is nearly 0.2 Å longer than the equatorial contact and a large decrease in the overlap population is expected. Indeed, the overlap does decrease from 0.526 to 0.360. Interestingly, though, the NCS is such a good donor that even for longer bond lengths the overlap is comparable to Mo–X_{eq} values, X = Cl or Br, and greater than any Mo–F overlap.

The last column of Table 3 presents the sum of all the Mo–L overlaps for each molecule. This sum is expected to give some indication of the overall metal–ligand donation leading to an analogy with the 'sum-rule' of cellular ligand field (c.l.f.) theory wherein the sum of all the c.l.f. e_λ parameters is related to the spherical component of the ligand-field potential and hence to the overall ligand-to-metal charge donation.[31] Given the similarity between the Mo–Cl and Mo–Br interactions already indicated above, it is probably not surprising that the overlap population sum varies as $[MoOF_5]^{2-} < [MoOCl_4(OH_2)]^- \approx [MoOCl_4]^- \approx [MoOBr_4(OH_2)]^- < [MoO(NCS)_5]^{2-}$.

Finally, it is of interest to examine the relative ligand σ- and π-donor roles in these complexes. The equatorial ligand p-orbital populations can be broken down into their individual component parts p_x, p_y and p_z relative to the global axis frame. The p_z function and one of either p_x or p_y, depending on the coordinates of the particular ligand, must then be projected first onto the Mo–X axis, to obtain the total p-orbital density

Table 4 Experimental (ref. 9) and calculated transition energies (cm^{-1}) for molybdenyl complexes. Assignments are indicated in parentheses except for 'Other bands' which are all c.t. unless otherwise stated. Band III corresponds to the computed $4d_{xy} \longrightarrow 4d_{z^2}$ transition energy

Complex	Method	Band 1	Band 2	Other bands	Band III
$[MoOCl_4]^-$	Exptl.	16 400 (d–d)	23 000 (d–d)	26 500, 28 000	
	DVXα	16 418 (d–d)	22 627 (d–d)	29 335,[c] 31 948[c]	31 165
	MSXα[a]	17 450 (d–d)	25 240 (d–d)		
	MSXα[b]	15 600 (d–d)	23 000 (c.t.)	23 300 (d–d)	37 000
			25 700 (c.t.)		
$[MoOCl_4(OH_2)]^-$	Exptl.	12 000 (d–d)	23 000 (d–d)	24 500, 26 500	
	DVXα	13 022 (d–d)[d]	22 461 (d–d)	26 509, 28 811[c]	35 553
$[MoOBr_4(OH_2)]^-$	Exptl.	14 000 (d–d)	20 380 (c.t.)	23 000, 25 000	
	DVXα	13 566 (d–d)[d]	20 228 (c.t.)	23 968, 26 449[c]	35 475
			20 413 (d–d)		
$[MoOF_5]^{2-}$	Exptl.	12 420 (d–d)	25 000 (d–d)	32 000, 33 000	
	DVXα	11 191 (d–d)	29 735 (d–d)	33 100,[c] 36 104	45 740
	MSXα[a]	8 890 (d–d)	34 460 (d–d)		
$[MoO(NCS)_5]^{2-}$	Exptl.	13 000 (d–d)	19 150 (c.t.)	21 500, 26 000	
	DVXα	13 520 (d–d)	18 232[c] (c.t.)	19 750,[c] 25 175	
			18 644 (c.t.)	20 321[c]	

[a] Ref. 13. [b] Ref. 11. [c] c.t. band would lead to multiplet structure. [d] Average of $9a_1 \longrightarrow 7b_1$ and $9a_1 \longrightarrow 7b_2$ transition energies. The actual splitting is less than 500 cm^{-1}.

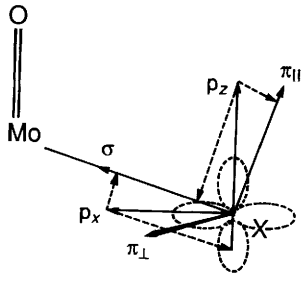

Fig. 3 Projection of p-orbital densities in a global *x*, *y*, *z* axis frame onto local Mo–X σ- and π-bonding directions

of σ symmetry, $\rho(\sigma_p)$, and secondly, perpendicular to the Mo–X axis, but in the plane containing the *z* axis, to obtain the total π density parallel to *z*, $\rho(\pi_{||})$ as shown in Fig. 3. The remaining p orbital contributes to π bonding perpendicular to the *z* axis $\rho(\pi_\perp)$. Adding the s-orbital population to $\rho(\sigma_p)$ gives the total σ population $\rho(\sigma)$. For an isolated halide, $\rho(\sigma)$, $\rho(\pi_{||})$ and $\rho(\pi_\perp)$ are 4, 2 and 2 respectively. Subtracting from these figures the relevant numbers for the complex and dividing by the number of M–L bonds gives a measure of the individual Mo–L σ, $\pi_{||}$ and $\pi_\perp$ charge donations relative to the isolated ligand. For $[MoOCl_4]^-$ the calculated values are 0.311, 0.146 and 0.064 while for $[MoOF_5]^{2-}$ they are 0.212, 0.081 and 0.062 respectively. The magnitude of Mo–Cl σ and $\pi_{||}$ donation is about half as much again as that for the Mo–F interaction, consistent with the generally larger donor role expected for Cl. However, the ratio of σ donation to the average π donation is 2.95:1 in both cases.

The constant σ/π ratio for Cl and F is unexpected. It is well known that F is higher in the spectrochemical series than Cl, yet F is lower in the nephelauxetic series.[32] Thus Cl should donate more strongly but give smaller ligand-field splittings. Within a ligand-field scheme like the c.l.f. model this result could be accommodated by larger e_σ and e_π parameters for Cl, thus implying greater donation, together with a decreasing e_σ/e_π parameter ratio to give smaller splittings. Unfortunately, any ligand-field analysis for these relatively high-symmetry complexes would be underdetermined so the DVXα predictions cannot be tested.

Another feature of the DVXα calculations is the apparent π-donor asymmetry, especially for Cl where $\rho(\pi_{||})$ is over twice as large as $\rho(\pi_\perp)$. A cylindrically symmetric π interaction is normally found for M–Cl bonding.[33] The DVXα scheme underestimates $\rho(\pi_\perp)$ for planar $[CuCl_4]^{2-}$ and perhaps here also. The source of this anomaly may be solid-state effects[34] but further study is required to investigate this suggestion fully.

Electronic Spectra.—The DVXα model gives consistently accurate reproduction of the absorption spectra of a variety of d^1 and d^9 metal complexes. The most recent work from this laboratory has yielded near-quantitative agreement with experimental band maxima for chlorocuprates,[20] $[CrOCl_4]^-$,[14] and several vanadium(IV) and VO^{2+} complexes.[15] Given the similarity between some of these complexes and the present MoO^{3+} species together with the relatively low spin–orbit coupling constant for Mo,[35] it is not surprising that the present DVXα calculations on MoO^{3+} species give excellent agreement with experiment also. Table 4 compares DVXα results with experiment and MSXα data.

The first absorption band is predicted to be a d–d absorption $^2B_2 \longrightarrow {}^2E$ corresponding to the one-electron promotion $4d_{xy} \longrightarrow 4d_{xz}$, $4d_{yz}$. This agrees well with experiment.[9] Moreover, there is a good correlation between the detailed shifts in the calculated and observed transitions. The DVXα results faithfully follow the changes in the experimental band energies from complex to complex. Reproduction of the second absorption feature is similarly impressive. Collison[9] has assigned this feature for $[MoOCl_4]^-$, $[MoOCl_4(OH_2)]^-$ and $[MoOF_5]^{2-}$ to the d–d transition $^2B_2 \longrightarrow {}^2B_1$ corresponding to the promotion $4d_{xy} \longrightarrow 4d_{x^2-y^2}$. The DVXα results concur. For $[MoOBr_4(OH_2)]^-$ and $[MoO(NCS)_5]^{2-}$, on the other hand, this band is assigned as charge transfer in origin.[9] Again the DVXα calculations concur. However, there is one point about the nature of the c.t. transition that deserves comment. Collison assigns these bands to in-plane-ligand to metal c.t. While the DVXα model predicts this assignment for $[MoOBr_4(OH_2)]^-$, the second absorption of $[MoO(NCS)_5]^{2-}$ actually arises from *axial* NCS→Mo transfer. Subsequent features above the second band invariably begin with some form of c.t. absorption. This is where the DVXα results again disagree slightly with Collison's assignments. Specifically, he assigns the 26 500 cm^{-1} feature of $[MoOCl_4]^-$ to the d–d transition $^2B_2 \longrightarrow {}^2A_1$ corresponding to the promotion $4d_{xy} \longrightarrow 4d_{z^2}$. The present DVXα calculations always place this d–d band above 30 000 cm^{-1}, contrary to Collison's assertion. Therefore, the feature at 26 500 cm^{-1} is probably better assigned as a Cl→Mo c.t. band for $[MoOCl_4]^-$.

Conclusion

The DVXα method has afforded excellent reproduction of the

electronic spectra of the d^1 oxometal complexes $[MoOCl_4]^-$, $[MoOCl_4(OH_2)]^-$, $[MoOBr_4(OH_2)]^-$, $[MoOF_5]^{2-}$ and $[MoO(NCS)_5]^{2-}$. In agreement with the most recent assignments,[9] the first band is predicted to be the d–d transition $^2B_2 \longrightarrow {}^2E$. Excellent reproduction of the energy variation of this band is obtained. The second band for $[MoOCl_4]^-$, $[MoOCl_4(OH_2)]^-$ and $[MoOF_5]^{2-}$ is also a d–d transition, as suggested by experiment,[9] while for $[MoOBr_4(OH_2)]^-$ and $[MoO(NCS)_5]^{2-}$ it is c.t. in origin. Significantly, this band is assigned as an *axial* ligand-to-metal c.t. transition for the NCS complex, contrary to the general assertion that these features arise from transitions involving the equatorial ligands. A further minor discrepancy is that the DVXα calculations on $[MoOCl_4]^-$ predict the third band (at 26 500 cm^{-1}) to be a c.t. transition. Collison's proposition[9] that this feature is a d–d band, in common therefore with $[VOCl_4]^{2-}$ and $[CrOCl_4]^-$, is not supported. Overall, however, the discrepancies between the DVXα results and the latest experimental data are minor, attesting, once again, to the utility of the DVXα method. Both experiment and theory for MO^{n+} are basically in accord and demonstrate the essential correctness of the original Ballhausen and Gray treatment.

Acknowledgements

The author thanks Dr. David Collison for making his experimental data available prior to publication.

References

1 F. A. Cotton and G. Wilkinson, *Advanced Inorganic Chemistry*, 5th edn., Wiley-Interscience, New York, 1988.
2 R. H. Holm, *Chem. Rev.*, 1987, **87**, 1401.
3 J. Bordas, R. C. Bray, C. D. Garner, S. Gutteridge and S. S. Hasnain, *Biochem. J.*, 1980, **191**, 499; R. L. Robson, *Nature (London)*, 1986, **322**, 388.
4 C. J. Ballhausen and H. B. Gray, *Inorg. Chem.*, 1962, **1**, 111.
5 H. B. Gray and C. R. Hare, *Inorg. Chem.*, 1962, **1**, 363.
6 C. D. Garner, I. H. Hillier, J. Kendrick and F. E. Mabbs, *Nature (London)*, 1975, **258**, 138.
7 D. Collison, B. Gahan, C. D. Garner and F. E. Mabbs, *J. Chem. Soc., Dalton Trans.*, 1980, 667.
8 D. Collison, *J. Chem. Soc., Dalton Trans.*, 1989, 1.
9 D. Collison, *J. Chem. Soc., Dalton Trans.*, 1990, 2999.
10 L. G. Vanquickenborne and S. P. McGlynn, *Theor. Chim. Acta*, 1968, **9**, 390.
11 J. Weber and C. D. Garner, *Inorg. Chem.*, 1980, **19**, 2206.
12 C. D. Garner, J. Kendrick, P. Lambert, F. E. Mabbs and I. H. Hillier, *Inorg. Chem.*, 1976, **15**, 1287.
13 K. K. Sunil, J. F. Harrison and M. T. Rogers, *J. Chem. Phys.*, 1982, **76**, 3087.
14 R. J. Deeth, *J. Chem. Soc., Dalton Trans.*, 1990, 365.
15 R. J. Deeth, *J. Chem. Soc., Dalton Trans.*, 1991, 1467.
16 R. G. Parr and W. Yang, *Density-Functional Theory of Atoms and Molecules*, Oxford University Press, New York, 1989; R. J. Deeth, B. N. Figgis and M. I. Ogden, *Chem. Phys.*, 1988, **121**, 115.
17 A. Rosen, D. E. Ellis, H. Adachi and F. W. Averill, *J. Chem. Phys.*, 1976, **65**, 3629.
18 F. W. Averill and D. E. Ellis, *J. Chem. Phys.*, 1973, **59**, 6412.
19 E. J. Baerends, D. E. Ellis and P. Ros, *Chem. Phys.*, 1973, **2**, 41.
20 R. J. Deeth, *J. Chem. Soc., Dalton Trans.*, 1990, 355.
21 R. S. Mulliken, *J. Chem. Phys.*, 1955, **23**, 1833, 1841.
22 J. C. Slater, *Quantum Theory of Molecules and Solids*, McGraw-Hill, New York, 1974, vol. 4.
23 C. D. Garner, L. H. Hill, F. E. Mabbs, D. L. McFadden and A. T. McPhail, *J. Chem. Soc., Dalton Trans.*, 1977, 853.
24 C. D. Garner, L. H. Hill, F. E. Mabbs, D. L. McFadden and A. T. McPhail, *J. Chem. Soc., Dalton Trans.*, 1977, 1202.
25 A. Bino and F. A. Cotton, *Inorg. Chem.*, 1979, **18**, 2710.
26 R. Mattes, K. Mennemann, N. Jackel, H. Rieskamp and H. J. Brockmeyer, *J. Less-Common Met.*, 1980, **76**, 199.
27 W. Clegg, *Acta Crystallogr., Sect. C*, 1987, **43**, 791.
28 A. Bencini and D. Gatteschi, *J. Am. Chem. Soc.*, 1983, **105**, 5535.
29 B. Delley and D. E. Ellis, *J. Chem. Phys.*, 1982, **76**, 1949.
30 G. S. Chandler, R. J. Deeth, B. N. Figgis and R. A. Phillips, *J. Chem. Soc., Dalton Trans.*, 1990, 1417.
31 R. G. Woolley, *Chem. Phys. Lett.*, 1985, **118**, 207.
32 C. J. Ballhausen, *Introduction to Ligand Field Theory*, McGraw-Hill, New York, 1962.
33 R. J. Deeth and M. Gerloch, *Inorg. Chem.*, 1985, **24**, 1754.
34 J. A. Aramburu, personal communication.
35 J. S. Griffith, *The Theory of Transition-Metal Ions*, Cambridge University Press, Cambridge, 1961.

Received 7th January 1991; *Paper* 1/00085C